J. Fluid Mech. (1966), *vol.* 26, *part* 2, *pp.* 369–392
Printed in Great Britain

Wind-generated waves in thin liquid films

By ALEX D. D. CRAIK
Department of Applied Mathematics, St Salvator's College,
University of St Andrews, Fife

(Received 11 October 1965)

In the presence of an air stream, a uniform liquid film on a horizontal flat plate may be unstable to small disturbances, and waves may arise. In this paper the hydrodynamic stability of thin liquid films is examined both experimentally and theoretically.

The experiments concern water films thinner than those which have been examined in the past. It is found that, when the film thickness is sufficiently *small*, a previously unknown type of instability occurs. The theoretical analysis explains this surprising phenomenon.

Due to interaction of the mean airflow and small disturbances of the liquid–air interface, normal and tangential stress perturbations are produced at the liquid surface. It is shown that small wave-like disturbances become unstable when the joint influence of the component of normal stress in phase with the wave elevation and the component of tangential stress in phase with the wave slope is sufficient to overcome the 'stiffness' of the liquid surface due to gravity and surface tension. It is found that the destabilizing role of the tangential stress component is dominant for very thin films, and that instability may occur whatever the velocity of the air stream, provided the film is made sufficiently thin.

1. Introduction

Experimental investigations of wind-generated waves in horizontal liquid films have been carried out by Hanratty & Engen (1957), van Rossum (1959) and Cohen & Hanratty (1965). In these, the thinnest films examined had thicknesses of about 0·05 cm. When the airflow is sufficiently large, instability arises in such films owing to the irreversible transfer of energy from the airflow to small surface disturbances. The theoretical stability problem for this case has been considered by Cohen & Hanratty (1965) and by Craik (1965).

Films of the type in question have moderately large Reynolds numbers, and may be regarded as systems with fairly low internal damping. For these, instability occurs when the viscous dissipation is insufficient to balance the energy transfer to a corresponding neutral wave. On the other hand, for films thinner than these, the Reynolds numbers are smaller and the internal damping is larger. Because of this increased internal damping, the 'dynamic' instability which arises in thicker films is less likely to occur in very thin films.

An experiment is described in § 2 which concerns water films thinner than those investigated previously. In this experiment a new type of instability was discovered, which is different in character from that observed in thicker films.

A theoretical investigation of the stability of such thin films occupies the remainder of this paper.

If turbulent fluctuations in the airflow may be disregarded, the undisturbed state of the system can be treated theoretically as one of two-dimensional plane parallel flow. As is customary in problems of this general type, the system is regarded as having an arbitrary small disturbance, the Fourier components of which are assumed to be dynamically independent. Since each Fourier component is a solution of the linearized equations of motion, it is sufficient to examine the behaviour of a general harmonic disturbance. Also, since every periodic three-dimensional disturbance may be treated in terms of a corresponding two-dimensional problem (see Lin 1955, §§3.1, 5.2), only two-dimensional harmonic disturbances need be considered.

In the presence of a prescribed harmonic disturbance of the air–liquid interface, the stresses exerted by the airflow upon the interface may always, in principle, be calculated. Thus, for a given airflow, a general relationship between the kinematical and stress conditions at the interface may be determined. This permits the formulation of the precise boundary conditions to be satisfied by the liquid film at the interface, for any small periodic disturbance. These boundary conditions, the equations of motion of the liquid and the two remaining boundary conditions at the rigid wall together constitute a complete boundary-value problem; and its solution yields a relationship between the properties of the primary flow and those of the disturbance. From this relationship may be deduced the conditions governing the occurrence of instability in the liquid film.

The present method, then, treats the problem in two parts: namely, an evaluation of the surface stresses exerted by the airflow upon a prescribed disturbance of the boundary, and the solution of the stability problem for the liquid film. As was indicated by Benjamin (1959), this method has considerable advantages over one in which the complete stability problem is posed for the system: the latter approach is likely to lead to great complexity, with an accompanying loss of physical insight.

Since the behaviour of the liquid film is largely governed by the stresses exerted upon its surface by the airflow, fairly precise estimates of these stresses are obviously desirable. In general, the air stream is turbulent, and, consequently, random fluctuations of stress exist at the liquid surface. However, although the resonant response of a liquid surface to random pressure fluctuations is an important process in the generation of ocean waves (see Phillips 1962), a resonance mechanism of this type is unimportant in the present problem. The reason for this is that the velocities of the convected fluctuations in the airflow are always much greater than the 'natural' wave velocities in liquid films, thus permitting only a very weak response of the surface.

The surface stresses produced by interaction of the mean airflow with small periodic perturbations of the bounding surface—here, the surface of the liquid film—have been evaluated by Miles (1957, 1959, 1962) and by Benjamin (1959) for mean air-velocity profiles of boundary-layer type. Although their 'quasi-laminar' flow model entirely neglects the turbulent fluctuations of the airflow, there is a considerable amount of experimental evidence that it gives a good

approximation to the actual pressure component in phase with the wave elevation (see Benjamin 1964). However, it has not yet been directly verified that this theory gives satisfactory estimates of the remaining (smaller) stress components. Indeed, the interaction between small surface perturbations and the turbulent fluctuations in the airflow might give rise to systematic surface stresses which are not negligible compared with those arising from interaction of the surface perturbations and the mean airflow.

In the stability problem to be examined, precise estimates are required for only two stress components, and one of these is the pressure component in phase with the wave elevation, for which the quasi-laminar model appears to be adequate. The second component required is that of tangential stress in phase with the wave slope. For lack of a better estimate of the latter component, that given by the quasi-laminar theory is used here; it seems reasonable to hope that this estimate is at least of the correct order of magnitude. In fact, the substitution of these precise estimates is delayed until a fairly advanced stage in the analysis, the surface stresses being represented until then by suitable parameters. This procedure facilitates the physical interpretation of the results.

The initial formulation of the stability problem for the liquid film has much in common with that of Miles (1960), which also concerns the stability of liquid films in uniform shearing motion. However, in the Miles analysis, the variable surface stresses exerted by the airflow were for the most part neglected; and instability occurred at large values of the liquid Reynolds number, due to transfer of energy from the primary liquid flow to the disturbance. In contrast to the Miles analysis, the present stability problem involves the solution of the Orr–Sommerfeld equation for fairly *small* values of the liquid Reynolds number, R. Also, for sufficiently thin films, the wavelengths λ of all relevant periodic disturbances are likely to be large compared with the film thickness h: it may therefore be assumed that the dimensionless wave-number $\alpha = 2\pi h/\lambda$ is small compared with unity.

A method of solving the Orr–Sommerfeld equation for small values of αR and of α^2 was employed by Benjamin (1957) to investigate the stability of a liquid film flowing down an inclined plane under gravity. This method expresses the solution as a series of ascending powers in αR and α^2. A rather different approach, due to Yih (1963), is equally applicable to the present problem, and might yield higher approximations more readily than Benjamin's method. In fact, Benjamin's method is used in the present paper, the amount of calculation being similar for both methods, to the degree of approximation required.

Theoretical results relating to the occurrence of instability in water films are deduced. These are found to be in general agreement with the experimental findings described in § 2.

The notation is fully explained in the text. However, the following selective list of symbols is provided for the convenience of readers.

The mean flow:

h	liquid film thickness;
V	velocity of air–liquid interface;
H	thickness of air phase;

U_0	maximum air velocity;
μ, μ_a	viscosities of liquid and air;
ρ, ρ_a	densities of liquid and air;
$\nu\,(=\mu/\rho),\ \nu_a\,(=\mu_a/\rho_a)$	kinematic viscosities of liquid and air;
$R = Vh/\nu$	Reynolds number of liquid;
$R_a = U_0 H/\nu_a$	Reynolds number of air;
U_i'	velocity gradient of air at liquid interface;
c_f	friction coefficient of airflow;
$\tau_0 = \mu_a U_i' = c_f \rho_a U_0^2$	mean tangential stress at interface.

The disturbance:

$k = 2\pi/\lambda$	dimensional wave-number;
c'	dimensional wave velocity (complex);
$\alpha = kh$	dimensionless wave-number;
$c = c_r + ic_i = c'/V$	dimensionless wave velocity;
$c_g = \partial(\alpha c_r)/\partial\alpha$	dimensionless group velocity;
$R_\alpha = U_0/k\nu_a$	air Reynolds number based on wave-number k.

Surface parameters:

$\eta(x,t) = \delta e^{i\alpha(x-ct)}$	vertical displacement of air–liquid interface;
$\sigma_{yy} = \Pi\eta(x,t)$	dimensionless normal stress perturbation (Π complex);
$\sigma_{xy} = \Sigma\eta(x,t)$	dimensionless tangential stress perturbation (Σ complex);
$P_r = (\rho V^2/h)\,\Pi_r$ $T_i = (\rho V^2/h)\,\Sigma_i$	dimensional stress parameters;
I, Δ, β, s	defined in (5.1a, b), (5.4);
g	gravitational acceleration;
γ	coefficient of surface tension;
$G = \tilde{G}/R^2 = gh/V^2$	(Froude number)$^{-1}$;
$T = \tilde{T}/R^2 = \gamma/\rho h V^2$	(Weber number)$^{-1}$;
k_c, Φ, h_c	defined in (9.3), (9.4), (9.5).

2. The experiment

2.1. *The apparatus*

The experiment was initially conducted in a closed rectangular channel 46 in. long, 11·4 in. wide and 6·0 in. high. The channel bottom consisted of a single sheet of plate glass, and the sides and top were of Plexiglas. A later modification reduced the channel height to 1·0 in. Throughout the experiment, the plate glass bottom was horizontal. A diagram of the apparatus is given in figure 1.

The airflow was provided by a large fan which drew air through the apparatus from the atmosphere. To straighten the flow, lengths of honeycomb grid were situated at either end of the channel; and, to reduce vibrations, the fan was connected to the channel by some flexible ducting. Airflow measurements were made by means of a Pitot-static tube, which could be inserted through a small hole in the top of the channel. This tube was mounted on a device which enabled alteration and accurate measurement of its height above the channel bottom.

Water was introduced into the channel from a reservoir situated in the entry section, in front of the bottom glass plate and behind the honeycomb grid. The

water was supplied to this reservoir from a head tank through a needle valve which permitted very fine adjustment of the flow rate. The reservoir contained a closely fitting piece of sponge rubber, from which the water exuded on to the plate. Interference with the airflow was kept at a minimum by ensuring that the surface of the sponge was level with the glass plate.

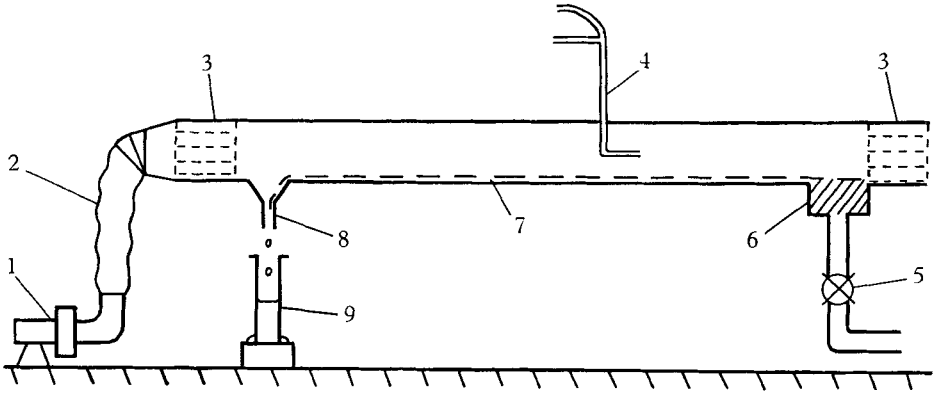

FIGURE 1. Diagram of apparatus (not to scale). 1, Fan; 2, flexible ducting; 3, honeycomb grid; 4, Pitot-static tube, attached to manometer; 5, needle valve controlling flow from head tank; 6, sponge-filled reservoir; 7, water film; 8, water exit; 9, measuring jar.

At the downstream end of the channel, the water flowed into a V-shaped reservoir fitted with an outlet which allowed the water to be collected in a measuring jar; by this means the flow rate could be determined. By careful levelling and scrupulous cleaning of the glass plate, very thin uniform water films could be maintained in the presence of an airflow.

Sections of 20 cm length were marked off in the channel by pieces of measuring tape fixed to the underside of the glass plate. The surface velocity of the water film could be found by sprinkling lycopodium powder on to the surface, then timing individual particles with a stopwatch as they traversed one or more of the sections. By taking measurements at several points across the width of the channel, the mean surface velocity could be determined graphically.

Since the surface of a uniform film was horizontal, the motion was independent of gravity. Also, since the ratio of film thickness to channel height was small, the pressure gradient required to maintain the airflow had negligible effect upon the velocity profile in the water film. Therefore, since the film was subject to a uniform shear stress, the velocity profile in the liquid was very nearly linear, and the mean velocity of the film was half the surface velocity. Since the surface velocity V, the volumetric flow rate Q and the channel width w are known, the mean film thickness h may be found from the expression $h = 2Q/Vw$.

2.2 *Observations*

When the airflow was kept constant, the effect of decreasing the liquid flow rate was to decrease the film thickness. For several constant values of the airflow, the

film thickness was decreased in this way from a fairly large value. The following is typical of the sequence of events observed in the channel of 1 in. height:

(i) A 'pebbled' surface occurred for thick films; (ii) regular waves travelling down the channel were obtained on decreasing the film thickness; (iii) these waves disappeared for still thinner films, leaving an essentially smooth surface; (iv) for very thin films, the surface again exhibited disturbances which are described below; (v) when the flow-rate was decreased still further, dry patches formed on the plate. More satisfactory results were obtained using the 1 in. channel than using the 6 in. one. For the latter, the air velocity could not be made sufficiently large to cause case (i), and the waves of case (ii) were much less well defined than in the 1 in. channel, making quantitative investigation impossible. Otherwise the results were similar. Photographs of cases (i) to (iv) are shown in figure 2 (i)–(iv) (plate 1). When the air velocity was sufficiently large, the stable régime (iii) disappeared, and disturbances of types (ii) and (iv) could occur simultaneously (see figure 3, plate 2). Cases (i), (ii) and (iii) correspond to three of the flow régimes observed in earlier experiments, but the additional unstable régime (iv) has not previously been investigated. For convenience, the waves of case (ii) will be called 'fast' waves and those of case (iv) 'slow' waves.

The 'fast' waves were straight-crested and apparently sinusoidal, with wavelengths of 1–2 cm, and their velocity of propagation was considerably larger than the velocity of the liquid surface. On the other hand, the 'slow' waves were of an obviously non-periodic nature, having comparatively steep fronts and long rear portions. These waves were slow moving, with velocities somewhat *less* than that of the liquid surface. The wave-crests extended over most of the width of the channel, and were generally curved concavely in the direction of motion (see figure 2 (iv), plate 1).

With a constant airflow, the amplitude of 'slow' waves increased as the mean film thickness was decreased. Unfortunately, no direct means of measuring local wave displacements was available; but local values could be obtained which were clearly several times greater than the mean film thickness. By use of lycopodium powder, the local surface velocity could be observed. On the long rear portions of the waves, this was somewhat larger than the mean surface velocity; but, in the vicinity of the crests, the velocity became very small, then again increased on the front portions.

Just after their inception, successive 'slow' waves were at least 10 cm apart, and sometimes as few as three or four crests occurred in the whole length of the channel. However, when the waves grew in amplitude, their spacing became irregular, due to the dependence of wave velocity on amplitude. At the high air velocities when 'fast' and 'slow' waves occurred together (figure 3, plate 2), the distances between the crests of both wave-types were reduced.

The stable film of case (iii) was almost mirror-smooth, the only disturbances of the surface being minute striations parallel to the direction of the airflow. The presence of these striations was observed also in cases (ii), (iv) and (v), but could not be detected in case (i) because of the intense agitation of the water surface. They were probably caused by small fast-moving eddies in the turbulent air stream: if so, their minute size confirms the view expressed in the introduction,

that the effect of random turbulent stresses is insignificant.

Measurement of the air velocity at various heights above the liquid surface revealed that the velocity profile closely resembled that for turbulent flow in a smooth-walled channel. The maximum velocity occurred almost midway between the water surface and the roof of the channel, there being no noticeable asymmetry of the velocity profile due to the different natures of the upper and lower boundaries.

Measurements were made of the conditions in the 1 in. channel giving rise to transition from 'pebbled' flow to two-dimensional 'fast' waves, and from 'fast' waves to a stable film. The transition from the stable régime to 'slow' waves was examined in both the 1 in. and 6 in. channels. The following procedure was adopted.

The airflow was set at a constant value, and the maximum air velocity was determined. The liquid flow rate was gradually decreased from a fairly large value, until the required transition occurred, and it was then measured. The mean surface velocity was found and the film thickness was calculated as described above. The wave velocity and corresponding surface velocity were also determined; but, for this, the flow rate had generally to be adjusted to a value slightly different from that at transition, in order to obtain sufficiently distinct waves. These observations were repeated for several values of the airflow.

The small disturbances which occurred near transition were best seen by viewing along the plane of the surface. For photographic purposes, the channel could be illuminated by a small floodlight placed beyond the honeycomb grid at the channel entrance. With this arrangement, very small disturbances of the surface cast a distinct 'shadow' upon a sheet of paper attached to the underside of the glass plate.

Results for the 1 in. channel are shown in figures 4–7 and in table 2, and those for the 6 in. channel are shown in table 1.

Air velocity U_0 (cm sec^{-1})	336	505	543	673	683
Film thickness h (cm)	0·0128	0·023	0·0218	0·0355	0·0307
Surface velocity V (cm sec^{-1})	0·355	0·73	0·85	1·7	1·7

TABLE 1. Transition to 'slow' waves in the 6 in. channel.

2.3. *Discussion of results*

In figure 4, the maximum air velocity U_0 is plotted against the velocity gradient V/h in the water film, and these results are compared with the corresponding curve for turbulent airflow through a smooth-walled channel.† The close agreement confirms that the velocity profile in the film is linear (and hence laminar): it also indicates that, to good approximation, the airflow over the water surface may be regarded as aerodynamically smooth.

† For a mean velocity profile which obeys the $\frac{1}{7}$th power law (see Schlichting 1960, p. 506), we have $U_0/v_* = 8{\cdot}74(Hv_*/2\nu_a)^{\frac{1}{8}}$, where H is the channel height, ν_a is the kinematic viscosity of air and v_* is the friction velocity. By definition, $\rho_a v_*^2$ equals the shear stress at the wall, which is here $\mu V/h$, ρ_a being the density of air and μ the viscosity of water. These results yield the relationship between U_0 and V/h shown in figure 4.

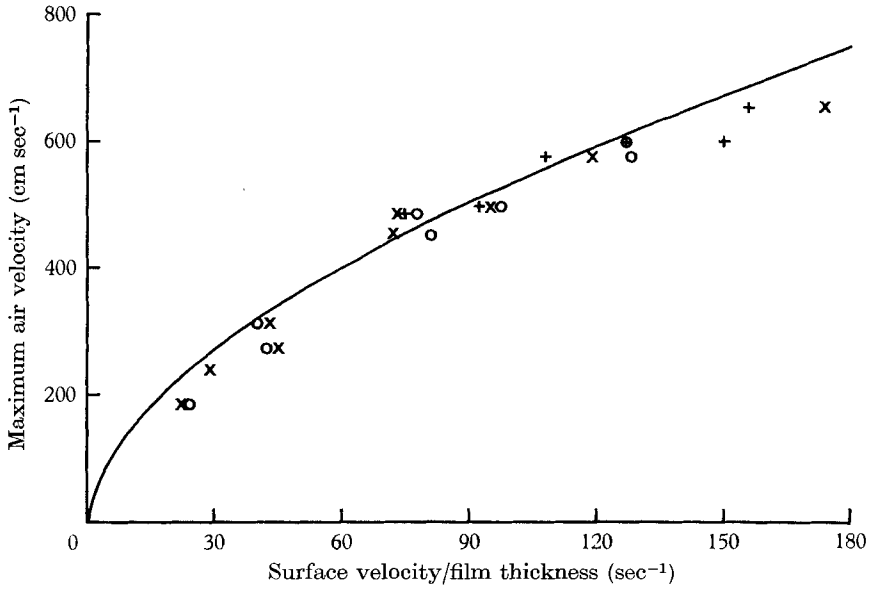

FIGURE 4. Maximum air velocity plotted against the ratio of surface velocity to film thickness. The points marked +, ○ and × denote conditions at transition between cases (i) and (ii), (ii) and (iii), (iii) and (iv) respectively.

In figure 5, the film thickness h is plotted against the maximum air velocity U_0 for the three transitions: while, in figure 6, the corresponding film Reynolds numbers $R = Vh/\nu$ are shown against the air Reynolds number $R_a = U_0 H/\nu_a$, where H is the channel height and ν, ν_a are the kinematic viscosities of water and air respectively.

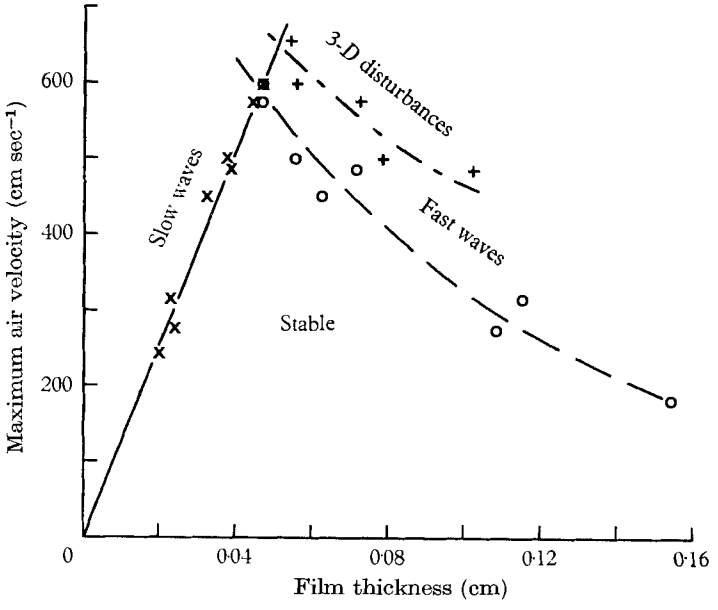

FIGURE 5. Maximum air velocity plotted against thickness of water film for the three transitions.

The most remarkable feature of these results—and of those for the 6 in. channel —is the appearance of 'slow' waves for all values of the air velocity, when the film thickness is made sufficiently small. (In fact, these waves were observed for air velocities considerably smaller than those recorded in figure 5, but quantitative results were unobtainable because of the difficulty of maintaining sufficiently thin, uniform films.) Thus, contrary to expectation, the thinnest films are not the most stable: instead, there is a non-zero thickness for which a water film is most stable. In the 1 in. channel, this thickness was about 0·046 cm.

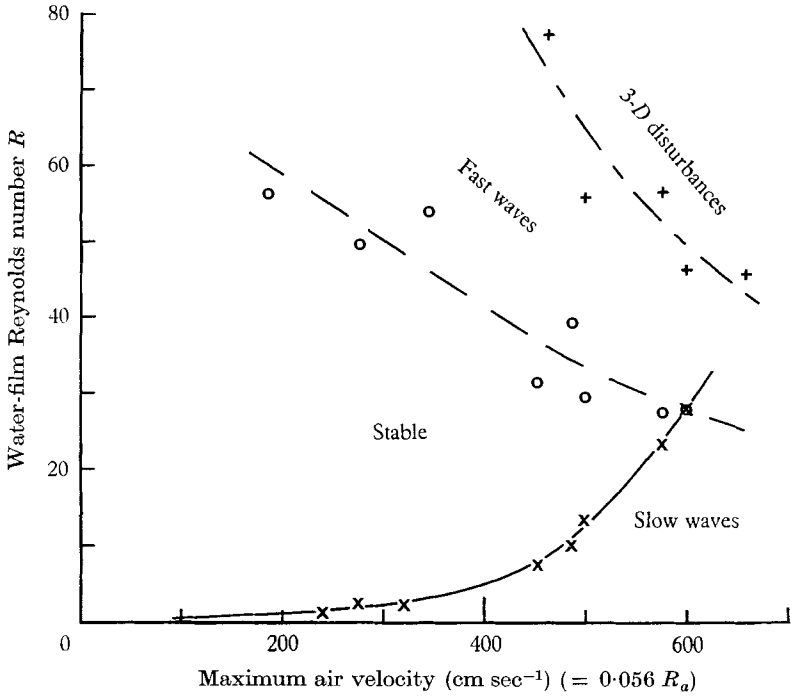

FIGURE 6. Reynolds number R of water film plotted against the maximum air velocity U_0 and the air-stream Reynolds number R_a, for the three transitions.

For 'slow' waves, corresponding wave velocities and surface velocities are shown in figure 7. The results plotted are for the smallest waves the velocities of which could be accurately determined; but, even for these, the amplitudes might not have been small compared with the mean film thickness. The points fall upon a straight line, the wave velocity always being slightly less than the surface velocity. 'Slow' waves of larger amplitude were observed to travel even more slowly, but quantitative measurements were not made, since the wave-amplitudes could not be determined. However, it was noticed that the velocities of these larger waves did not become less than half the mean surface velocity, except when the film thickness was clearly non-uniform across the width of the channel. (For the largest waves, localized dry patches frequently formed in front of the crests, disrupting the uniformity of the film.)

For 'fast' waves just beyond the transition from a stable film, the variations of surface velocity and wave velocity with film thickness are shown in table 2. Unfortunately, the accuracy to which these larger wave velocities could be determined by direct observation was somewhat restricted by the shortness of the channel.

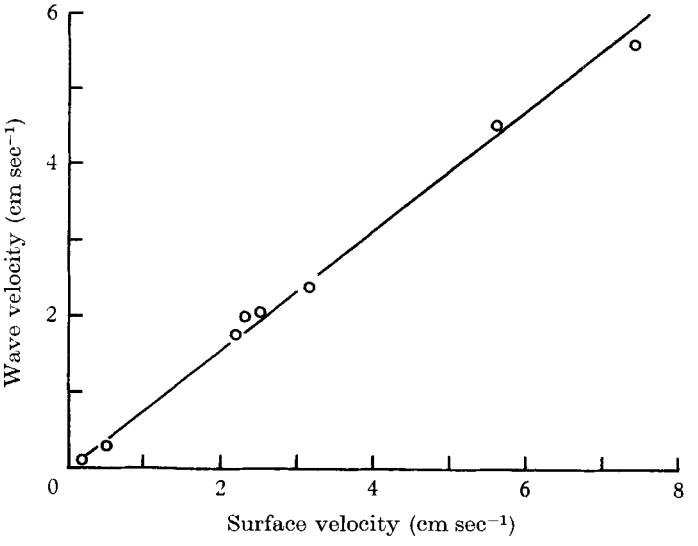

FIGURE 7. Velocity of 'slow' waves plotted against surface velocity of water film.

Since the experiment was designed to investigate very thin films, the results for 'slow' waves are much more accurate than those for 'fast' waves. In particular, there is a considerable spread in the results for the transitions from stable films to 'fast' waves, and from 'fast' waves to three-dimensional disturbances. In contrast, the transition from stable films to 'slow' waves was sharply defined.

Film thickness h (cm)	0·0535	0·0665	0·082	0·086	0·12	0·154
Surface velocity V (cm sec^{-1})	6·8	6·45	6·67	6·65	5·1	3·63
Wave velocity c' (cm sec^{-1})	11·9	12·0	12·0	12·8	19·6	—

TABLE 2. Properties of 'fast' waves just beyond transition from stable film.

3. The primary flow

In the following theoretical analysis, all quantities are made dimensionless relative to the film thickness h, the velocity of the liquid surface V and the liquid density ρ. The Reynolds number of the film is defined as $R = Vh/\nu$, where ν is the kinematic viscosity of the liquid. The motion of the liquid is assumed to be laminar; and, because of the mean tangential stress exerted by the air stream, the basic velocity profile in the liquid is taken to be linear. The primary motion of the liquid is related to that of the air by the equation

$$\mu(V/h) = \mu_a U_i', \tag{3.1}$$

which expresses continuity of tangential stress across the interface. Here

$\mu\,(=\rho\nu)$ and μ_a are the viscosity coefficients for the liquid and air respectively, and U_i' is the dimensional vertical velocity gradient of the airflow at the interface.

Dimensionless co-ordinates x and y are chosen such that the direction of flow is parallel to the x-axis, and the positions of the rigid wall and the undisturbed liquid surface are denoted by the planes $y=-1$ and $y=0$ respectively. The dimensionless primary velocity profile in the liquid is then

$$\bar{u}(y) = 1+y. \tag{3.2}$$

A sketch of this configuration is given in figure 8.

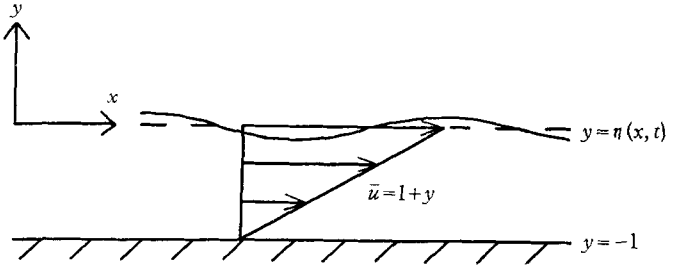

FIGURE 8. Sketch of shear flow and surface disturbance.

4. The stability problem

The nomenclature used is similar in many respects to that of Miles (1960). A two-dimensional wavelike perturbation of the liquid surface is represented by

$$y = \eta(x,t) = \delta e^{i\alpha(x-ct)},$$

where α is the (real) dimensionless wave-number and c is the dimensionless wave velocity, which may be complex. The wave amplitude is assumed to be sufficiently small for the problem to be linearized.

The continuity equation may be satisfied by introducing the perturbation stream function

$$\psi(x,y,t) = -\phi(y)\,\eta(x,t),$$

such that the perturbation velocity components are

$$u = \psi_y = -\phi'\eta, \quad v = -\psi_x = i\alpha\phi\eta, \tag{4.1a,b}$$

where the prime denotes differentiation with respect to y. Substituting (3.2) and (4.1a,b) into the linearized Navier–Stokes equations, we obtain

$$\phi^{\mathrm{iv}} - 2\alpha^2\phi'' + \alpha^4\phi = i\alpha R(1+y-c)(\phi''-\alpha^2\phi), \tag{4.2}$$

$$p = [(1+y-c)\phi' - \phi - (i\alpha R)^{-1}(\phi''' - \alpha^2\phi')]\,\eta(x,t), \tag{4.3}$$

$$\tau = R^{-1}(u_y + v_x) = -R^{-1}(\phi'' + \alpha^2\phi)\,\eta(x,t), \tag{4.4}$$

where p and τ are the perturbations of pressure and of shear stress respectively. Result (4.2) is the Orr–Sommerfeld equation in the form appropriate for the present velocity profile.

Since the perturbation velocity components must vanish at the wall, two boundary conditions are

$$\phi(-1) = \phi'(-1) = 0. \tag{4.5a,b}$$

Also, the linearized kinematic condition at the liquid surface is

$$v = D\eta/Dt = \eta_t + \eta_x, \quad y = 0;$$

that is,

$$\phi(0) = 1 - c. \tag{4.6}$$

The two remaining boundary conditions concern the normal and tangential stresses at the air–liquid interface. We define the parameters Π and Σ, which are generally complex, by

$$\sigma_{yy} = \Pi\eta(x,t), \quad \sigma_{xy} = \Sigma\eta(x,t), \tag{4.7}$$

where σ_{yy} and σ_{xy} are the dimensionless normal and tangential stress perturbations exerted at the interface by the air stream. The condition for continuity of tangential stress at the interface is

$$\tau = \sigma_{xy}, \quad y = 0;$$

or, on using results (4.4), (4.6) and (4.7),

$$\phi'' + [\alpha^2 + R\Sigma(1-c)^{-1}]\phi = 0, \quad y = 0. \tag{4.8}$$

The condition that the capillary and gravitational forces resisting displacement and the normal stresses on either side of the interface should be in equilibrium is

$$-p + 2R^{-1}v_y = T\eta_{xx} + (\Pi - G)\eta, \quad y = 0;$$

the parameters G and T being defined as

$$G = gh/V^2, \quad T = \gamma/\rho h V^2,$$

where g is gravitational acceleration and γ is the coefficient of surface tension at the interface. The quantities G^{-1} and T^{-1} are seen to be the Froude and Weber numbers of the film. On using (4.1*a*, *b*), (4.3) and (4.6), this condition becomes

$$(1-c)\phi' - \phi - (i\alpha R)^{-1}(\phi''' - 3\alpha^2\phi') - (T\alpha^2 + G - \Pi)(1-c)^{-1}\phi = 0, \quad y = 0. \tag{4.9}$$

Apart from an arbitrary amplitude factor, the linearized characteristic-value problem is completely specified by the fourth-order differential equation (4.2) and the four boundary conditions (4.5*a*, *b*), (4.8) and (4.9). The requirement that all four boundary conditions should be satisfied yields an eigenvalue equation for c, from which may be deduced the conditions governing the stability of the film.

5. The surface stresses

The results to be described are taken from Benjamin's paper (1959), which incorporates the earlier work of Miles (1957) and extends it by the inclusion of first-order viscous terms. For convenience, reference is made to Benjamin's paper by use of the parentheses $\langle\ \rangle$ containing the appropriate page or equation number. In later work, Miles (1962) has developed a method for calculating the

surface stresses, which is free from many of the approximations implicit in the estimates given here. However, Benjamin's estimates may be expressed in simple analytic form, and are sufficient for present purposes.

The estimates were derived for flows with dimensional velocity profiles $U(y)$, which tend to some constant value U_0 as y becomes large. For flow over a rigid wavy boundary (i.e. with $c = 0$), the results ⟨7.11⟩, ⟨7.12⟩ and ⟨2.13⟩ give the following expressions for the normal and tangential stress parameters Π and Σ:

$$\Pi = \frac{\rho_a}{\rho}\left(\frac{U_0}{V}\right)^2 I\alpha(1 - 1{\cdot}288\, e^{\frac{1}{6}\pi i}\Delta) + 2i\alpha\left(\frac{\mu_a U_i'}{\rho V^2}\right),$$

$$\Sigma = 1{\cdot}372\, e^{\frac{1}{3}\pi i}\frac{\rho_a}{\rho}\left(\frac{U_0}{V}\right)^2 I\alpha^{\frac{5}{3}}\left(\frac{U_i' h^2}{\nu_a}\right)^{-\frac{1}{3}},$$

where
$$\Delta = I\alpha^{\frac{4}{3}}\left(\frac{U_0}{U_i' h}\right)^2\left(\frac{U_i' h^2}{\nu_a}\right)^{\frac{1}{3}}, \quad I = \int_0^\infty (U/U_0)^2 e^{-\alpha y}\, d(\alpha y). \qquad (5.1a, b)$$

(Additional factors of I are included in the expressions for Σ and Δ; since, on ⟨p. 198⟩, Benjamin shows that the estimates are thereby improved. A misprint in ⟨7.12⟩ gives the exponent of Σ as $\frac{1}{6}\pi i$ instead of $\frac{1}{3}\pi i$.) Use of (3.1) and the relationship $\nu_a U_i' = c_f U_0^2$, where c_f is the friction coefficient, yields the results

$$\Pi = (\alpha/Rc_f)\,[I - \sqrt{3}\, s + i(2c_f - s)], \qquad (5.2)$$

$$\Sigma = (2\beta I/\sqrt{3}\, c_f)\, e^{\frac{1}{3}\pi i}\alpha^3(\alpha R)^{-\frac{4}{3}}, \qquad (5.3)$$

where
$$s = 0{\cdot}644\Delta I, \quad \Delta = (I/c_f)\,(\mu_a/\mu)^{\frac{2}{3}}(\alpha R)^{-\frac{2}{3}}\alpha^2,$$

$$2\beta/\sqrt{3} = 1{\cdot}372(\nu_a/\nu)^{\frac{2}{3}}(\rho_a/\rho)^{\frac{1}{3}}. \qquad (5.4)$$

The term $\alpha I/Rc_f$ in Π is independent of the air viscosity, and could be derived from the (linearized) inviscid equations of motion for the air. On the other hand, the remaining terms in Π, and the entire contribution to Σ, depend explicitly on the air viscosity, since they are due to viscous Reynolds stresses near the boundary. (Since the boundary is rigid, with $c = 0$, there is no contribution to Π due to inviscid Reynolds stresses in the critical layer where $U(y)$ equals c.)

Since σ_{yy} equals $\Pi\eta$ and σ_{xy} equals $\Sigma\eta$, the real parts of Π and Σ correspond to components of normal and tangential stress which are in phase with the wave displacement $\eta(x,t)$, while the imaginary parts of Π and Σ denote stress components which are in phase with the wave slope $\partial\eta/\partial x$.

The accuracy of the above estimates depends on the validity of several assumptions about the nature of the airflow. These assumptions mainly concern the relative magnitudes of various length-scales of the problem, which are: the wavelength of the disturbance, the effective boundary-layer thickness, the width of the region near the boundary where the velocity profile is approximately linear, and the thickness of the 'wall friction layer' within which viscosity has an appreciable effect on the flow perturbation. A full discussion of these assumptions is given by Craik (1965). There, it is also shown that the results (5.2) and (5.3) may be applicable to turbulent airflows in a channel of finite height H, provided the wavelength of the disturbance is not large compared with the channel height: i.e. provided $\alpha H/h \geqslant O(1)$. In this case, the mean velocity profile

$U(y)$ is symmetrical, and U_0 is redefined as the maximum velocity in the centre of the channel: also, the upper limit of infinity for the integral I is replaced by the channel height H.

The range of validity of results (5.2) and (5.3) is best indicated in terms of the air-stream Reynolds number $R_\alpha = U_0 h/\alpha\nu_a$ based on the wave-number of the disturbance. If the viscous sublayers adjacent to the walls occupy only a small fraction of the channel height, the mean air velocity profile is typically of the form

$$\begin{aligned} U(y)/U_0 &= (2yh/H)^{\frac{1}{7}}, \quad 0 < y < H/2h, \\ &= \left[2\left(1-\frac{yh}{H}\right)\right]^{\frac{1}{7}}, \quad \frac{H}{2h} < y < \frac{H}{h}. \end{aligned} \tag{5.5}$$

For this velocity profile, for values of c_f which are $O(10^{-3})$, and for $\alpha H/h \geqslant O(1)$, all but one of the conditions on the validity of the results (5.2) and (5.3) are found to be fairly well satisfied when R_α is $O(10^3)$, $O(10^4)$ and, possibly, $O(10^5)$. The exception is the condition that Δ should be small compared with unity, which is satisfied only if R_α is not less than about 10^4 (unless I is small, when values of $O(10^3)$ might suffice).

When the wavy disturbance has a small (dimensional) velocity c' relative to the material surface, the stresses are similar to those exerted on a rigid boundary: in the present example, this is so when the condition $c'/U_0 \leqslant O(10^{-1})$ is satisfied (see Benjamin ⟨p. 182⟩ and Craik 1965). Also, the results are applicable to a liquid surface, provided the periodic horizontal velocity component at the surface is not large (see ⟨pp. 171–2⟩). Both these conditions are well satisfied in the present problem.

In brief, if the role of turbulent fluctuations may be neglected—which is by no means certain—the estimates (5.2) and (5.3) might apply to turbulent flows in a channel over a considerable range of the Reynolds number R_α. Unfortunately, justification for using these estimates to denote the stresses in the experiment described in § 2 is not as readily forthcoming as one might wish: for, there, R_α was typically $O(10^3)$, and therefore the condition that Δ should be small was not well satisfied.

6. The governing equations

The Orr–Sommerfeld equation (4.2) may be re-written as

$$\phi^{\mathrm{iv}} = (\hat{p}+\hat{q}y)\phi'' - (\hat{r}+\hat{q}y)\alpha^2\phi, \tag{6.1}$$

where $\hat{p} = i\alpha R(1-c)+2\alpha^2, \quad \hat{q} = i\alpha R, \quad \hat{r} = i\alpha R(1-c)+\alpha^2.$

Following Benjamin's method of solution, we replace ϕ in (6.1) by the series

$$\phi(y) = \sum_{n=0}^{\infty} A_n y^n,$$

where the A_n are constants. This leads to the recurrence relation

$$\begin{aligned} &n(n-1)(n-2)(n-3)A_n \\ &\quad = (n-2)(n-3)\hat{p}A_{n-2} + (n-3)(n-4)\hat{q}A_{n-3} - \alpha^2(\hat{r}A_{n-4} + \hat{q}A_{n-5}), \end{aligned} \tag{6.2}$$

by which $\phi(y)$ may be expressed as a series of ascending powers in y, with the parameters αR and α^2 also occurring in successive powers. The resultant expression contains the four disposable constants A_0, A_1, A_2 and A_3.

If the conditions

$$\alpha^2 \ll 1, \quad \alpha R < O(1), \quad \alpha R|c| < O(1) \qquad (6.3a,b,c)$$

are satisfied, the series for ϕ converges very rapidly, and only the first few terms need be considered. For simplicity, the following analysis is confined to cases where these conditions hold. The recurrence relation (6.2) then yields the approximate expression

$$\phi(y) = A_0 + A_1 y + A_2(y^2 + \tfrac{1}{12}\hat{p}y^4 + \tfrac{1}{60}\hat{q}y^5) + A_3(y^3 + \tfrac{1}{20}\hat{p}y^5 + \tfrac{1}{60}\hat{q}y^6), \qquad (6.4)$$

where terms of the second and higher orders of small quantities have been omitted from each of the coefficients of $A_{0,1,2,3}$.

On replacing ϕ by this expression in the boundary conditions (4.5a,b), (4.8) and (4.9), the following set of equations is obtained:

$$\begin{aligned}
A_0 - A_1 + A_2(1 + \tfrac{1}{12}\hat{p} - \tfrac{1}{60}\hat{q}) - A_3(1 + \tfrac{1}{20}\hat{p} - \tfrac{1}{60}\hat{q}) &= 0,\\
A_1 - A_2(2 + \tfrac{1}{3}\hat{p} - \tfrac{1}{12}\hat{q}) + A_3(3 + \tfrac{1}{4}\hat{p} - \tfrac{1}{10}\hat{q}) &= 0,\\
A_0[\alpha^2 + R\Sigma(1-c)^{-1}] + 2A_2 &= 0,\\
A_0 i\alpha R[1 + (T\alpha^2 + G - \Pi)(1-c)^{-1}] - A_1(\hat{p} + \alpha^2) + 6A_3 &= 0.
\end{aligned}$$

Excluding the trivial case $A_{0,1,2,3} = 0$, it is evident that these four equations are consistent only when the determinant of the coefficients of $A_{0,1,2,3}$ is zero. In evaluating this determinant, terms of the second and higher powers of $\hat{p}$ and $\hat{q}$ may be neglected by virtue of conditions (6.3a,b,c), leading to the result

$$T\alpha^2 + G - \Pi + \frac{3i\Sigma}{2\alpha} = (1-c)\left\{\frac{3}{i\alpha R} + \frac{6}{5}(1-c) - \frac{7}{8} + \frac{27}{5}\frac{\alpha^2}{i\alpha R}\right\}, \qquad (6.5)$$

where terms of order αR, α^2, ΣR and $\Sigma\alpha$ have been omitted. This equation determines c as a function of α, R and the surface properties represented on the left-hand side.

Equation (6.5) is a quadratic in $(1-c)$ with the solution

$$(1-c) = \xi \pm \{\xi^2 + \tfrac{5}{6}[T\alpha^2 + G - \Pi + (3i\Sigma/2\alpha)]\}^{\frac{1}{2}},$$

where

$$\xi = \tfrac{35}{96} + (5i/4\alpha R)(1 + \tfrac{9}{5}\alpha^2).$$

However, it is desirable to examine the real and imaginary parts of c separately, and we therefore write

$$c = c_r + ic_i, \quad \Pi = \Pi_r + i\Pi_i, \quad \Sigma = \Sigma_r + i\Sigma_i.$$

On separating the real and imaginary parts of (6.5), we obtain

$$\tfrac{6}{5}(c_r - 1)^2 + \tfrac{7}{8}(c_r - 1) - (c_i/\alpha R)(3 + \tfrac{27}{5}\alpha^2 + \tfrac{6}{5}\alpha R c_i) = T\alpha^2 + G - \Pi_r - (3\Sigma_i/2\alpha), \qquad (6.6)$$

$$c_i\{\tfrac{12}{5}(c_r - 1) + \tfrac{7}{8}\} + \{(c_r - 1)/\alpha R\}(3 + \tfrac{27}{5}\alpha^2) = -\Pi_i + (3\Sigma_r/2\alpha). \qquad (6.7)$$

7. The stability condition

For neutrally stable disturbances, c_i is zero, and equations (6.6) and (6.7) simplify to

$$\tfrac{6}{5}(c_r-1)^2+\tfrac{7}{8}(c_r-1) = T\alpha^2+G-\Pi_r-(3\Sigma_i/2\alpha), \tag{7.1}$$

$$(c_r-1)\,(3+\tfrac{27}{5}\alpha^2) = \alpha R\{-\Pi_i+(3\Sigma_r/2\alpha)\}. \tag{7.2}$$

Also, when $\frac{1}{3}\alpha R|\Pi_i|$ and $\frac{1}{2}R\Sigma_r$ are small compared with unity, (7.1) and (7.2) yield the simple approximate results

$$T\alpha^2+G-\Pi_r-(3\Sigma_i/2\alpha) = 0, \tag{7.1a}$$

$$c_r = 1. \tag{7.2a}$$

Expressed in dimensional variables, these results are

$$\rho g+\gamma k^2 = P_r+(3T_i/2kh), \tag{7.1b}$$

$$c' = V, \tag{7.2b}$$

where c', k are the dimensional wave velocity and wave-number, and P_r, T_i are the dimensional stress parameters, defined by

$$P_r = (\rho V^2/h)\,\Pi_r, \quad T_i = (\rho V^2/h)\,\Sigma_i.$$

We note that P_r and T_i are independent of the properties of the liquid film.

When c_i is non-zero, the rate of amplification or damping may be found from (6.6) and (6.7). In particular, when $|\alpha c_i R| \ll 1$, equation (6.7) gives the approximate result $c_r = 1$; and substitution of this value in (6.6) yields

$$\alpha c_i R = \frac{(\alpha R)^2}{3}\left[\Pi_r+\frac{3\Sigma_i}{2\alpha}-T\alpha^2-G\right], \tag{7.3}$$

when small terms are neglected. The corresponding dimensional amplification is

$$\sigma = \frac{V}{h}(\alpha c_i) = \frac{(kh)^2}{3\mu}\left[P_r+\frac{3T_i}{2kh}-\gamma k^2-\rho g\right]. \tag{7.3a}$$

When $|\alpha c_i R|$ is not small compared with unity, the wave velocity c_r is found, from (6.7), to be

$$c_r-1 = \frac{-\frac{7}{8}(\alpha c_i R)-\alpha R\Pi_i+\frac{3}{2}R\Sigma_r}{3+\frac{27}{5}\alpha^2+\frac{12}{5}\alpha c_i R},$$

and, when $\alpha R|\Pi_i|$, $R\Sigma_r$ and α^2 are all much less than unity, this simplifies to

$$c_r-1 = \frac{-\frac{7}{24}}{(\alpha c_i R)^{-1}+\frac{4}{5}}. \tag{7.4}$$

The conditions (7.1*b*) and (7.2*b*) for neutral stability do not depend upon the existence of a basic shear flow in the liquid. (In fact, equation (7.1*b*) may be derived very simply by neglecting the primary flow throughout.) Equation (7.2*b*) states that the wave travels with the velocity of the fluid particles comprising the surface, and (7.1*b*) expresses the balance of forces at the surface.

It is seen from (7.3*a*) that instability occurs when

$$P_r+(3T_i/2kh) > \rho g+\gamma k^2; \tag{7.5}$$

that is, when the effect of the surface stresses is sufficient to overcome the

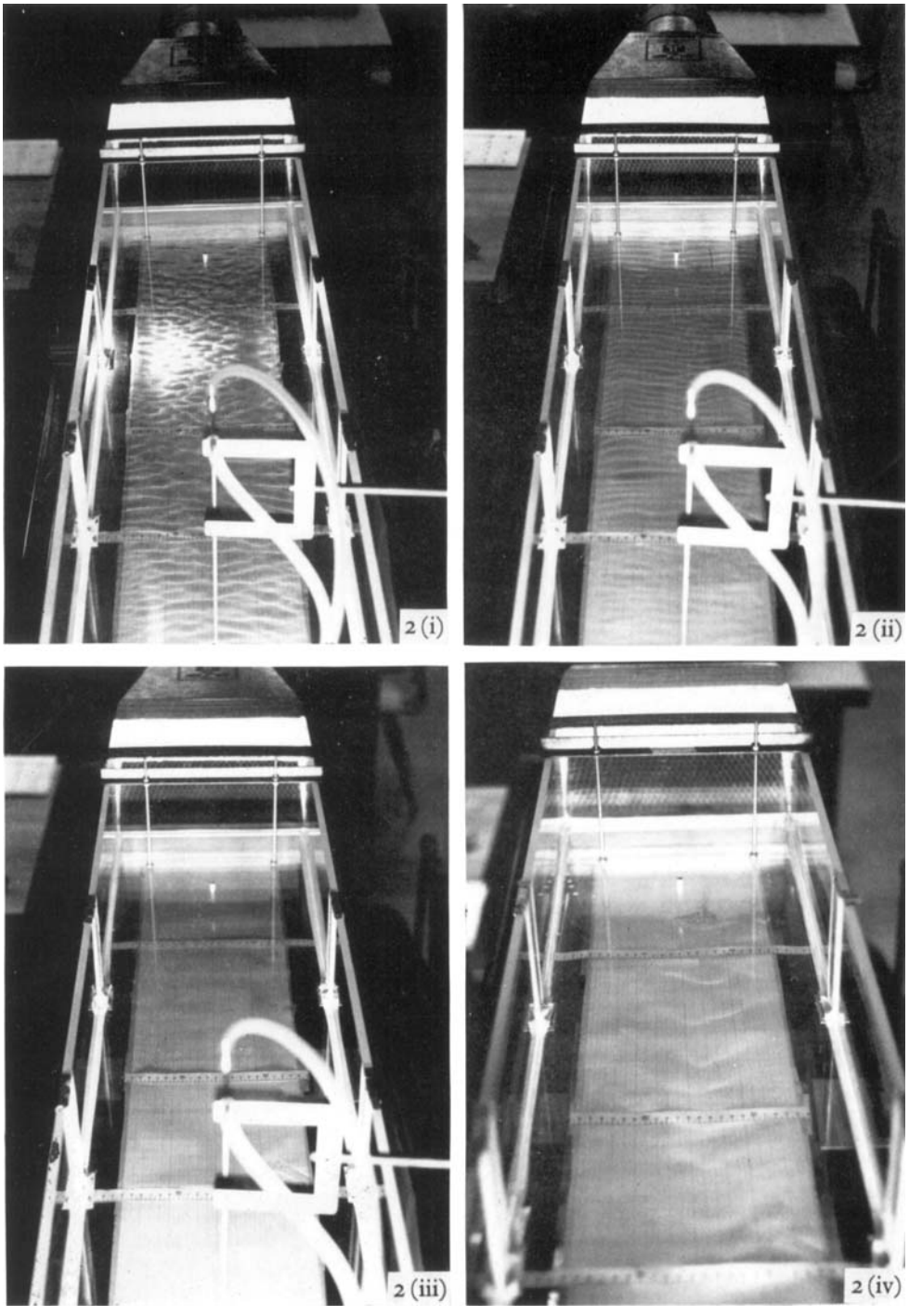

FIGURE 2. (i) Pebbled flow. (ii) 'Fast' waves. (iii) Stable film. (iv) 'Slow' waves.

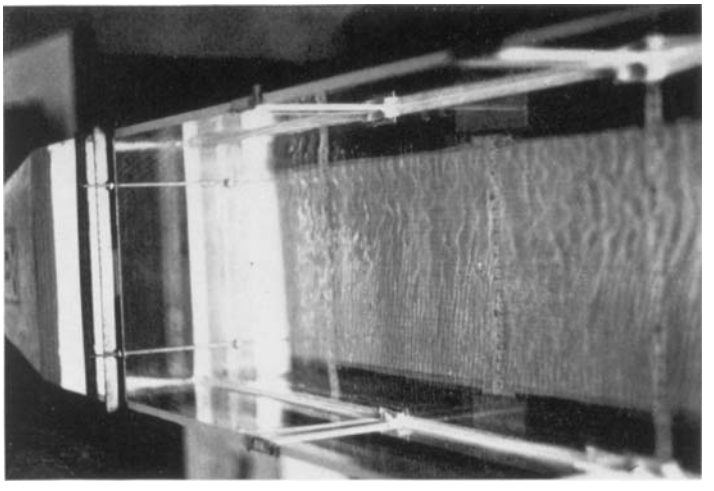

FIGURE 3. 'Fast' and 'slow' waves at large air velocity.

restoring forces of gravity and surface tension. Although P_r is generally much greater than T_i, the effect of the variable shear stress cannot be neglected when kh is small; indeed, the term in T_i becomes dominant for sufficiently small values of kh. Because of this, instability must always occur in sufficiently thin films, whatever the magnitude of the airflow. Thus, with a given airflow, instability can always be induced in an initially stable film by decreasing its thickness. These results are in qualitative agreement with the experimental findings of §2.

The physical explanation of this surprising phenomenon is as follows. The component of normal stress represented by P_r or Π_r is in phase with the wave displacement, and it attempts to deform the liquid surface by exerting an upwards force upon the crests and a downwards force upon the troughs of small periodic disturbances. Also, the tangential-stress component represented by T_i or Σ_i is in phase with the wave slope, and it has the effect of accelerating the liquid on the windward slopes while retarding that on the leeward slopes. The latter mechanism tends to displace fluid towards the crests and away from the troughs of existing small disturbances, thereby increasing their amplitude. The thinner the film, the more effective is this mechanism: for, in very thin films, the perturbation velocity component in the horizontal direction is much greater than that in the vertical, and the influence of the variable tangential stress extends throughout the whole film. The development of unstable disturbances is governed by continuity considerations. Their growth rate is proportional to the rate of accumulation of liquid near the crests; and this, in turn, is inversely proportional to the liquid viscosity, in agreement with result (7.3 a).

The present type of instability is entirely different from that likely to occur in thicker films. For films with moderately large Reynolds numbers, instability is due to the *irreversible* transfer of energy from the mean airflow to the disturbance through the stress components represented by Π_i and Σ_r. More precisely, instability occurs when the viscous dissipation within the film is less than the energy transfer to a corresponding neutral wave; and such energy transfer can only take place through *non-conservative* forces. These forces are provided by the normal stress component in phase with the wave slope and the tangential stress component in phase with the wave displacement.

In contrast, for films with small Reynolds numbers, the stress components which cause instability are those represented by Π_r and Σ_i, both of which act *conservatively* on the wave. Unlike that for thicker films, this type of instability is virtually independent of the irreversible processes of viscous dissipation and energy transfer through the stress components Π_i and Σ_r. In this respect, it is similar to 'Kelvin–Helmholtz' instability. (These two distinct types of instability fall within the threefold classification of unstable disturbances proposed by Benjamin (1963). The instability of moderately thick films usually belongs to class B, while that of thin films belongs to class C.)

8. The stability curves

In order to proceed further, we must introduce the precise expressions for Π_r and Σ_i given in (5.2) and (5.3). Since these estimates are good approximations only when Δ is small—that is, when s is small compared with I—sufficiently

accurate representations are

$$\Pi_r = \alpha I/Rc_f, \quad \Sigma_i = (\beta I/c_f)\alpha^3(\alpha R)^{-\frac{4}{3}}. \tag{8.1 a,b}$$

Since the value of I varies only slightly with considerable changes in α, the quantities I/c_f and β may be regarded as constants which depend on the properties of the airflow.

It is convenient to introduce the new parameters $\tilde{G}$ and $\tilde{T}$, defined as

$$\tilde{G} = R^2G = gh^3/\nu^2, \quad \tilde{T} = R^2T = \gamma h/\rho\nu^2. \tag{8.2 a,b}$$

These parameters have the advantage that they remain constant for a liquid film whose thickness is unchanged, even though its surface velocity—and hence its Reynolds number—may vary. If, for example, curves of neutral stability are found which correspond to fixed values of $\tilde{G}$ and $\tilde{T}$, each of these is the neutral curve *for a liquid film of constant thickness*. If suitable pairs of values for $\tilde{G}$ and $\tilde{T}$ are chosen, stability curves may be obtained over a range of film thicknesses, for any liquid.

On using results (8.1 *a,b*) and (8.2 *a,b*), the condition (7.1 *a*) for neutral stability becomes

$$\tilde{T}\alpha^2 + \tilde{G} = (I/c_f)\,[\alpha R + \tfrac{3}{2}\beta(\alpha R)^{\frac{2}{3}}], \tag{8.3}$$

and the neutral curves of R against α may be found by assigning appropriate values to $\tilde{G}$, $\tilde{T}$, I/c_f and β. Likewise, curves of constant amplification may be calculated from equation (7.3), which now takes the form

$$\{3(\alpha c_i R)/\alpha^2\} + \tilde{T}\alpha^2 + \tilde{G} = (I/c_f)\,[\alpha R + \tfrac{3}{2}\beta(\alpha R)^{\frac{2}{3}}]. \tag{8.4}$$

Since the dimensional amplification σ equals $(\alpha c_i R)\nu/h^2$, such curves have constant values of $\alpha c_i R$.

For given values of R, the wave-number of the most unstable disturbance may be found from (8.4) by equating $\partial(\alpha c_i R)/\partial\alpha$ to zero. This yields the result

$$4\tilde{T}\alpha^2 + 2\tilde{G} = (I/c_f)\,[3\alpha R + 4\beta(\alpha R)^{\frac{2}{3}}]. \tag{8.5}$$

For air over water, β is approximately 0·76; also, a typical value for I/c_f is 220 (corresponding to, say, $I \simeq 0{\cdot}6$ and $c_f \simeq 2{\cdot}7 \times 10^{-3}$). With these values, together with those for $\tilde{T}$ and $\tilde{G}$ corresponding to a water film of thickness 0·0215 cm and kinematic viscosity 0·01 $\mathrm{cm^2\,sec^{-1}}$, curves of constant amplification were calculated from equation (8.4) for $\alpha c_i R$ equal to 0, 0·01, 0·02 and 0·1. Also, the curve denoting the most unstable mode was found from (8.5).

To facilitate comparison with experiment, the results are presented as curves of dimensional wave-number $k\,(=\alpha/h)$ against the mean dimensional shear stress τ_0, the latter being a property of the airflow alone. The shear stress τ_0 is related to the Reynolds number of the film and to the maximum air velocity U_0 by the expressions

$$\tau_0 = (\mu^2/\rho h^2)R = \rho_a c_f U_0^2.$$

The curves are shown in figure 9, the dashed curve being that for the most unstable disturbance. For neutral disturbances, the minimum critical value of τ_0 is 0·89 $\mathrm{g\,cm^{-1}\,sec^{-2}}$, and the corresponding wave-number is 3·0 $\mathrm{cm^{-1}}$.

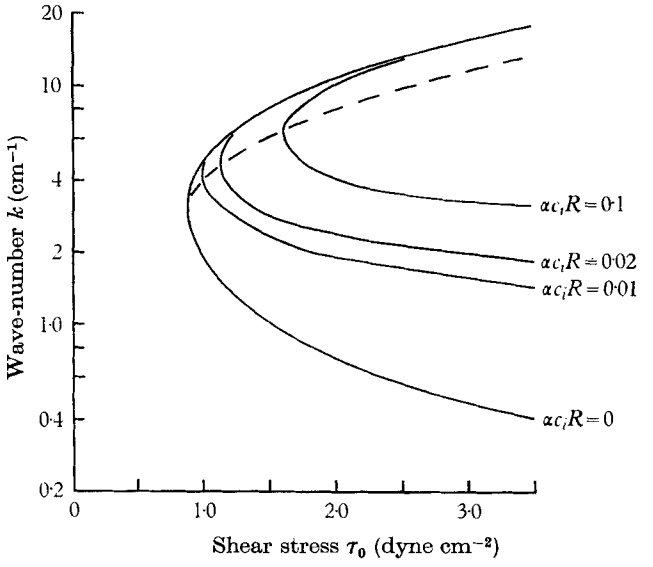

FIGURE 9. Wave-number k plotted against mean shear stress τ_0 at several constant values of the dimensionless amplification $\alpha c_i R$, for a water film of thickness 0·0215 cm, and $I/c_f = 220$. The curve ———— denotes the most unstable disturbance.

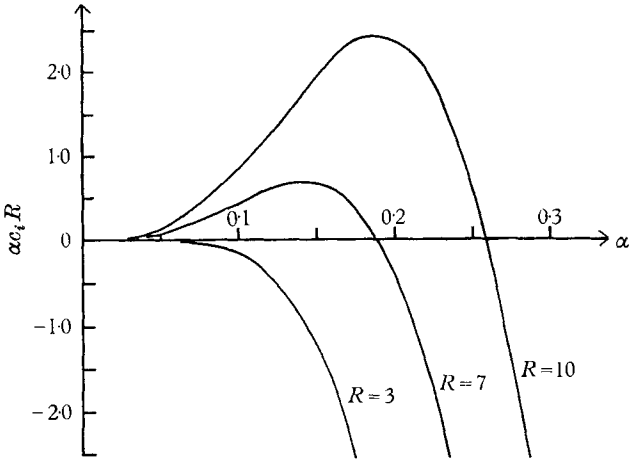

FIGURE 10. Dimensionless amplification $\alpha c_i R$ plotted against dimensionless wave-number α, for water films of thickness 0·02 cm with $R = 3$, 7, 10, and for $I/c_f = 220$.

With the same values of I/c_f and β as above, but with values of $\tilde{T}$ and $\tilde{G}$ corresponding to a water film of thickness 0·02 cm, the variation of the amplification $\alpha c_i R$ with wave-number α was found for three values of the Reynolds number: $R = 3$, 7 and 10. These three curves are shown in figure 10. Although αR and $\alpha c_i R$ are somewhat larger than unity for part of these curves, their values never exceed 3, and the curves probably remain reasonable approximations.

Figures 9 and 10 both reveal that the wave-number of the most unstable mode increases considerably for values of the shear stress (or Reynolds number) beyond the critical.

9. The critical case

In dimensional quantities, equation (7.1 *b*) is

$$g+\frac{\gamma}{\rho}k^2=\frac{I}{c_f}\left\{\frac{k\tau_0}{\rho}+\frac{3\beta\nu^{\frac{2}{3}}}{2h}\left(\frac{k\tau_0}{\rho}\right)^{\frac{2}{3}}\right\},$$

which may be re-written to express h in terms of k and τ_0, as

$$\left(\frac{3I}{2c_f}\beta\nu^{\frac{2}{3}}\right)\frac{1}{h}=\left(\frac{k\tau_0}{\rho}\right)^{-\frac{2}{3}}\left\{g+\frac{\gamma}{\rho}k^2-\frac{I}{c_f}\left(\frac{k\tau_0}{\rho}\right)\right\}. \tag{9.1}$$

Now, $\partial h/\partial k$ vanishes when

$$\frac{4\gamma}{\rho}k^2-\frac{I}{c_f}\frac{\tau_0}{\rho}k-2g=0, \tag{9.2}$$

and only one root of this quadratic in k is positive. It is easily shown that $\partial^2(h^{-1})/\partial k^2$ is positive at this root. Thus, for a prescribed value of τ_0, there is a wave-number $k=k_c$ given by (9.2) for which h has a maximum value h_c. This value h_c is the critical film thickness above which all disturbances are damped for the given value of τ_0.

If, alternatively, the value of h is prescribed, it may be shown from (9.1) that $\partial\tau_0/\partial k$ vanishes at $k=k_c$. The value of τ_0 at k_c is the minimum shear stress τ_{0c} capable of sustaining undamped disturbances in a film of thickness h. The critical values τ_{0c}, h_c and k_c are now examined in more detail.

The root of equation (9.2) that is greater than zero is

$$k_c=(g\rho/2\gamma)^{\frac{1}{2}}[\Phi+\sqrt{(1+\Phi^2)}], \tag{9.3}$$

where

$$\Phi=\frac{\tau_{0c}}{\rho}\frac{I}{8c_f}\left(\frac{2\rho}{g\gamma}\right)^{\frac{1}{2}}. \tag{9.4}$$

It is seen that Φ is a dimensionless parameter whose value is determined by the properties of the airflow, and which is proportional to the mean shear stress τ_{0c}. On substituting for k_c in (9.1), the expression for h_c becomes

$$\frac{h_c}{\beta}\left(\frac{c_f g}{2I\nu^2}\right)^{\frac{1}{3}}=\frac{\Phi^{\frac{2}{3}}[\Phi+\sqrt{(1+\Phi^2)}]^{\frac{2}{3}}}{\frac{1}{2}-\Phi^2-\Phi\sqrt{(1+\Phi^2)}}=F(\Phi). \tag{9.5}$$

The function $F(\Phi)$ is plotted against Φ in figure 11.

As Φ increases from 0 to $2^{-\frac{3}{2}}$, $F(\Phi)$ and hence h_c increase monotonically from 0 to ∞. Accordingly, all liquid films for which the present theory remains valid are unstable when Φ exceeds $2^{-\frac{3}{2}}$. This is so because, with Φ greater than $2^{-\frac{3}{2}}$, there is a range of wave-numbers for which the normal-stress parameter Π_r is itself greater than the sum of the gravitational and surface-tension terms, $(G+T\alpha^2)$.

As Φ increases from 0 to $2^{-\frac{3}{2}}$, k_c increases monotonically from $(g\rho/2\gamma)^{\frac{1}{2}}$ to $(g\rho/\gamma)^{\frac{1}{2}}$. Thus, for water, where $\gamma/\rho\simeq 73\,\mathrm{cm^3\,sec^{-2}}$, k_c lies between 2·59 and 3·66 $\mathrm{cm^{-1}}$.

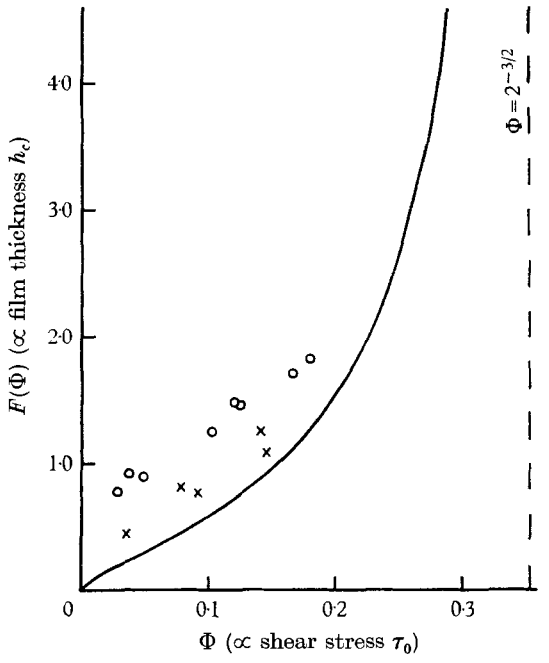

FIGURE 11. The function $F(\Phi)$ plotted against Φ, with experimental results for the 1 in. channel (denoted by ○) and for the 6 in. channel (denoted by ×).

10. Discussion of approximations

Conditions (6.3 a, b, c) restrict the range of validity of the theory to cases where $\alpha^2 \ll 1$ and $\alpha R < O(1)$. However, these conditions are not sufficient if the approximate equations (7.1 a) and (7.2 a) are used. In the present problem $|\Pi_i|$ is generally small compared with $3\Sigma_r/2\alpha$, and may be disregarded. Therefore, from (7.2), $(c_r - 1)$ is nearly equal to $\frac{1}{2}R\Sigma_r$. Now, result (7.1 a) is a good approximation to the stability condition (7.1) only if $\frac{7}{8}(c_r - 1)$ and $\frac{6}{5}(c_r - 1)^2$ are small compared with $3\Sigma_i/2\alpha$. On using result (5.3), it follows that these terms are sufficiently small provided

$$\alpha R \ll 6, \quad \alpha^2(\alpha R)^{\frac{2}{3}} \ll 15c_f/\beta I. \qquad (10.1\,a, b)$$

With β equal to 0·76 for air over water, and with I/c_f typically about 200, condition (10.1 b) requires that $\alpha^2(\alpha R)^{\frac{2}{3}} \ll 0{\cdot}1$. Clearly, both conditions are satisfied for sufficiently thin films.

The greatest film thickness for which 'slow' waves were observed was about 0·05 cm, and the critical wave-number predicted by theory is about 3 cm^{-1}. For such a film, the critical value of α is around 0·15: also, from figure 6, the critical value of R is found to be about 30, giving a value of nearly 4·5 for αR. Because of condition (10.1 a), this is a rather doubtful case; but, for thinner films, the values of α^2 and αR decrease rapidly. Thus, for a film of thickness 0·035 cm, the corresponding critical values are $\alpha \simeq 0{\cdot}1$ and $\alpha R \simeq 0{\cdot}75$. It is clear that, for films of this thickness or less, there is a range of α, including the critical wave-number, for which the conditions (6.3 a, b, c) and (10.1 a, b) are satisfied.

The only remaining doubt concerns the validity of the estimates (8.1 a, b) for the surface-stress parameters. The possible effects of turbulence have already been mentioned; and, even neglecting these, the results (8.1 a, b) do not adequately represent the stresses in all experimental situations. In particular, they are unlikely to provide accurate estimates of the stresses experienced in the experimental channels described in § 2. However, even in such cases, the results seem likely to be of the correct order of magnitude.

11. Comparison with experiment

The above analysis concerns only the temporal development of spatially uniform disturbances. However, the results are directly related to those for the spatial development of disturbances uniform in time. For, Gaster (1962) has shown that, provided the growth rates are small, the spatial amplification of disturbances uniform in time is approximately equal to the temporal amplification of spatially uniform disturbances with the same frequency, divided by the group velocity. Consequently, although the waves occurring in experiment are usually spatially amplified, the above results should remain applicable for these.

To compare the above theoretical results with those for the 'slow' waves described in § 2, we require values of I and c_f appropriate for the two experimental channels. On taking the wave-number k to be 3 cm^{-1}, and using the air-velocity profile (5.5) in the expression (5.1 b), the value of I is found to be about 0·6 for the 1 in. channel, and 0·37 for the 6 in. channel. Values of c_f for the 1 in. channel may be found from figure 4 by use of the result $c_f = \mu V/\rho_a U_0^2 h$. The actual value changes slowly with the air velocity, but $c_f = 3{\cdot}2 \times 10^{-3}$ may be taken as typical. For the 6 in. channel, a similarly obtained estimate is $c_f = 1{\cdot}5 \times 10^{-3}$.

On substitution of these values, together with $\beta = 0{\cdot}76$, into (9.4) and the left-hand side of equation (9.5), it is found that, for the 1 in. channel,

$$\Phi = 5{\cdot}1 \times 10^{-7} U_0^2, \quad F(\Phi) = 39 h_c,$$

and, for the 6 in. channel,

$$\Phi = 3{\cdot}15 \times 10^{-7} U_0^2, \quad F(\Phi) = 36 h_c,$$

where U_0 and h_c are measured in c.g.s. units. By using these results, the experimental measurements of h_c against U_0 have been plotted in figure 11, where they may be compared with the theoretical curve of $F(\Phi)$ against Φ.

In view of the approximate nature of the estimates for the surface-stress parameters, theory and experiment are in reasonable agreement. The displacement of the experimental results from the theoretical curve is greater for the 1 in. channel than for the 6 in. one; and, in all cases, the observed critical film thickness is larger than that given by theory. This last result suggests that the expression (8.1 b) underestimates the magnitude of the variable tangential-stress component Σ_i.

Result (7.2 b) shows that the dimensional wave velocity of neutral disturbances equals the surface velocity of the liquid film, and this result also holds for waves

of small amplification. Further, since c_r is virtually independent of α, the group velocity $c_g = c_r + \alpha(\partial c_r/\partial\alpha)$ is very nearly equal to c_r. In view of this, a non-periodic infinitesimal wave suffers very little dispersion (provided its wave-number spectrum is effectively all at small values of α); in particular, a long wave composed of a narrow band of wave-numbers near the optimum value for which $\alpha c_i R$ is a maximum will propagate with little change in form, but will undergo overall amplification at the rate $\alpha c_i R$. The observed instability, consisting of a succession of apparently independent humps, would appear to be of this general character. Since these waves were clearly non-periodic, the distance between successive crests bears no relation to the predicted critical wavelength of about 2 cm.

It is seen from figure 7 that the experimental wave velocities lie closely upon the line $c_r = 0{\cdot}8$. This result agrees reasonably well with theory, but it is desirable that the consistent deviation should be explained. Since the wave velocity, and hence the group velocity, of amplified disturbances is less than that for neutral waves, it is tempting to conclude that this deviation occurred because the observed disturbances were growing in amplitude. In fact, it may be shown from equation (7.4) that c_r attains the experimental value of 0·8 when $\alpha c_i R$ equals 1·7.

However, there is a more likely explanation of this deviation. We recall that the results plotted in figure 7 correspond to the smallest disturbances for which the velocities could be determined accurately, but that the velocities of larger disturbances were less than these. Because of the small thickness of the experimental films ($< 0{\cdot}05$ cm), it seems likely that the amplitudes of even the smallest disturbances were not small compared with the film thickness when their velocities were measured. If this were so, their wave velocities would be modified by non-linear effects. An examination by Craik (1965) of such finite-amplitude disturbances has revealed that the non-linear effects are likely to reduce the wave velocity, in agreement with observation.

I should like to thank Dr T. Brooke Benjamin for his guidance and helpful criticism throughout the course of this work. My thanks are due also to Dr W. Debler and Mr W. Huizenga of the University of Michigan for their part in the design and construction of the experimental apparatus described in § 2.

REFERENCES

BENJAMIN, T. BROOKE 1957 Wave formation in laminar flow down an inclined plane. *J. Fluid Mech.* **2**, 554.

BENJAMIN, T. BROOKE 1959 Shearing flow over a wavy boundary. *J. Fluid Mech.* **6**, 161.

BENJAMIN, T. BROOKE 1963 The threefold classification of unstable disturbances in flexible surfaces bounding inviscid flows. *J. Fluid Mech.* **16**, 436.

BENJAMIN, T. BROOKE 1964 Fluid flow with flexible boundaries. General lecture, 11*th Internat. Congr. Appl. Mech., Munich.* Berlin: Springer.

COHEN, L. S. & HANRATTY, T. J. 1965 Generation of waves in the concurrent flow of air and a liquid. *A.I.Ch.E. J.* **11**, 138.

CRAIK, A. D. D. 1965 Wind-generated waves in liquid films. Ph.D. Dissertation, University of Cambridge.

GASTER, M. 1962 A note on the relation between temporally-increasing and spatially-increasing disturbances in hydrodynamic stability. *J. Fluid Mech.* **14**, 222.

HANRATTY, T. J. & ENGEN, J. M. 1957 Interaction between a turbulent air stream and a moving water surface. *A.I.Ch.E. J.* **3**, 299.

LIN, C. C. 1955 *The Theory of Hydrodynamic Stability*. Cambridge University Press.

MILES, J. W. 1957 On the generation of surface waves by shear flows. *J. Fluid Mech.* **3**, 185.

MILES, J. W. 1959 On the generation of surface waves by shear flows, Part 2. *J. Fluid Mech.* **6**, 568.

MILES, J. W. 1960 The hydrodynamic stability of a thin film of liquid in uniform shearing motion. *J. Fluid Mech.* **8**, 593.

MILES, J. W. 1962 On the generation of surface waves by shear flows, Part 4. *J. Fluid Mech.* **13**, 433.

PHILLIPS, O. M. 1962 Resonant phenomena in gravity waves. *Proc. Symposia in Appl. Math.* **13**, 91.

SCHLICHTING, H. 1960 *Boundary Layer Theory*. New York: McGraw-Hill.

VAN ROSSUM, J. J. 1959 Experimental investigations of horizontal liquid films. *Chem. Engng Sci.* **11**, 35.

YIH, C.-S. 1963 Stability of liquid flow down an inclined plane. *Phys. Fluids* **6**, 321.